Coupled Systems Mechanics, *Vol. 2, No. 3 (2013) 215-230*
DOI: http://dx.doi.org/10.12989/csm.2013.2.3.215

Pull-in instability of electrically actuated poly-SiGe graded micro-beams

Xiao L. Jia*[1], Shi M. Zhang[1], Jie Yang[2] and Sritawat Kitipornchai[3]

[1]*College of Mechanical and Transportation Engineering, China University of Petroleum-Beijing, 18 Fuxue Road, Changping, Beijing, CO 102249, China*
[2]*School of Aerospace, Mechanical and Manufacturing Engineering, RMIT University, PO Box 71, Bundoora, VIC 3083 Australia*
[3]*School of Civil Engineering, The University of Queensland, Brisbane, St Lucia 4072, Australia*

(Received May 24, 2013, Revised July 18, 2013, Accepted July 24, 2013)

Abstract. This paper investigates the pull-in instability of functionally graded poly-SiGe micro-beams under the combined electrostatic and intermolecular forces and temperature change. The exponential distribution model and Voigt model are used to analyze the functionally graded materials (FGMs). Principle of virtual work is used to derive the nonlinear governing differential equation which is then solved using differential quadrature method (DQM). A parametric study is conducted to show the significant effects of material composition, geometric nonlinearity, temperature change and intermolecular Casimir force.

Keywords: functionally graded materials; micro-beam; pull-in instability; temperature change; Casimir force

1. Introduction

Recently, devices in micro-electro-mechanical-systems (MEMS) are typically designed to operate in one or more energy domains due to their unique advantages such as small size, lower power consumption, lower operation cost, increased reliability and higher precision. Therefore, numerous analytical, numerical and experimental studies have been conducted on the pull-in instability of the MEMS devices (Legtenberg and Tilmans 1994, Tilmans and Legtenberg 1994, Abdel-Rahman *et al.* 2002, Batra *et al.* 2006, 2008b).

It is known that a conventional MEMS device made of a single layer material is almost impossible to simultaneously meet all material and operational requirements. Most recently, the use of functionally graded materials (FGMs) in MEMS structures has been proposed (Craciunescu and Wuttig 2003, Fu *et al.* 2003). FGMs offer many advantages including improved stress distribution, enhanced thermal resistance, higher fracture toughness, and reduced stress intensity factors that make them very attractive in many engineering applications (Birman and Byrd 2007). Witvrouw and his co-workers (Witvrouw and Mehta 2005, Gromova *et al.* 2006) developed a multilayer poly-SiGe deposition process for fabricating MEMS structural layers that fulfill all material and economical requirements.

* Corresponding author, Ph.D., E-mail: xljia@cup.edu.cn

http://www.techno-press.org/?journal=csm&subpage=7 ISSN: 2234-2184 (Print), 2234-2192 (Online)

of functionally graded MEMS due to heat generated by an electric current. Jia *et al.* (2010, 2011) first studied the pull-in instability of electrostatically actuated FGM micro-beams allowing for geometric nonlinearity and intermolecular Casimir force, but without considering the temperature change. Mohammadi-Alasti *et al.* (2011) investigated the mechanical behavior of a cantilever FGMs micro-beam subjected to a nonlinear electrostatic pressure and a temperature change. Their study showed that due to variable thermal expansion coefficient along the thickness, a temperature change results in the deflection of FGM micro-beam. Nabian *et al.* (2013) and Sharafkhani *et al.* (2012) studied the stability of the rectangular and circular FGM micro-plates respectively. However, the two important factors—geometric nonlinearity and intermolecular force were neglected.

This paper investigates the pull-in instability of fixed poly-SiGe graded micro-beams under a combined action of electrostatic force, intermolecular Casmir force and a temperature change within the framework of von Karman nonlinearity and Euler-Bernoulli beam theory. The nonlinear pull-in results of the micro-beam are obtained by using the differential quadrature method (DQM). The effects of temperature change, material composition, geometrical nonlinearity and intermolecular Casimir force are discussed in detail through a parametric study. To the authors' best knowledge, no previous studies which cover all these issues are available.

2. FGM beam model

Shown in Fig. 1 is the structure of a typical micro-switch where the key components are a fixed electrode modeled as a ground plane and a movable electrode modeled as a poly-SiGe graded micro-beam of length L, width b, and thickness h, separated by a dielectric spacer with an initial gap g_0. The origin of the x-coordinate is taken to be the left end of the movable electrode whose deflection is denoted by w. The deflection of the micro-beam is caused by:

- Electrostatic force induced by an applied voltage,
- Intermolecular Casimir force,
- Temperature change.

The axial force due to residual strain from fabrication process is denoted by N_a and is positive for a tensile force. Under the influence of temperature change and/or the application of a driving voltage V_0, the micro-beam deflects towards the ground electrode under the action of a distributed electrostatic force F_e, Casmir force F_c and/or thermal strain. Both F_e and F_c are nonlinear functions of the gap $g(x) = g_0 - w(x)$ between the deformed micro-beam and the ground electrode.

When the voltage increases beyond a critical value, the movable electrode becomes unstable and collapses to the fixed electrode. This phenomenon, known as pull-in instability, is a subject of prime importance in the design of NEMS devices (Mobki *et al.* 2013). In this paper, we define the critical temperature variation when the micro-beam collapses only subjected to temperature change as "pull-in temperature variation", and the critical voltage corresponding to the micro-beam under the application of V_0 and temperature change as "pull-in voltage". The pull-in deflection denotes the critical deflection when the micro-beam collapses.

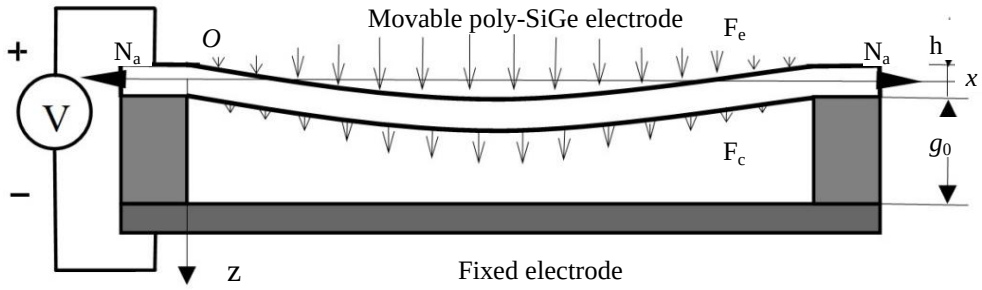

Fig. 1 An MEMS device with a poly-SiGe graded electrode

Table 1 Material properties of Germanium and Silicon

Material	E(GPa)	ν	α^* (K^{-1})
Ge	155	0.26	5.9×10^{-6}
Si	188	0.26	2.6×10^{-6}

*α: thermal expansion coefficient at 293K(20℃)

Taking into account the first-order fringing field correction, the electric field force per unit length can be written as (Gupta 1997, Huang *et al.* 2001)

$$F_e = \frac{\varepsilon_0 b V_0^{\,2}}{2\left[g_0(x)-w\right]^2} + \frac{0.65\varepsilon_0 V_0^2}{2\left[g_0(x)-w\right]} \tag{1}$$

where $\varepsilon_0 = 8.854\times10^{-12}\ \mathrm{C^2N^{-1}m^{-2}}$ is the permittivity of vacuum. The Casimir force takes the form of (Lamoreaux 2005)

$$F_c = \frac{\pi^2 \bar{h} c b}{240\left[g_0(x)-w\right]^4} \tag{2}$$

in which $\bar{h} = 1.055\times10^{-34}\,\mathrm{Js}$ is Planck's constant divided by 2π and $c = 3\times10^8\,\mathrm{ms^{-1}}$ is the speed of light.

The functionally graded poly-SiGe micro-beam is a mixture of germanium (Ge) as material phase 1 whose volume fraction is V_1, and silicon (Si) as material phase 2 whose volume fraction is V_2. Their material properties are listed in Table 1.

The mixing ratio of the FGMs changes smoothly and continuously along the thickness direction, and $V_1 + V_2 = 1$. Based on the exponential distribution model, the Young's modulus and thermal expansion coefficient of the beam vary in the thickness only (Erdogan and Wu 1997)

$$E(z) = E_b e^{\gamma(z-h/2)}, \quad \alpha(z) = \alpha_b e^{\lambda(z-h/2)} \tag{3}$$

where E_b and α_b are the values of the Young's modulus and thermal expansion coefficient at the bottom surface ($z = h/2$) of the beam respectively, γ and λ corresponds to the constants defining the material property variation along the thickness direction. Note that $\gamma = 0$ and $\lambda = 0$ correspond a special case where the beam is homogenous. In this paper, the bottom surface of the beam is 100% silicon. Poisson's ratio ν is taken to be constant since its influence is quite limited (Erdogan and Wu 1997).

To determine the material properties at the top surface ($z = -h/2$) of the micro-beam, the Voigt model is used, by which the effective material properties P_t at the top surface such as Young's modulus E_t and thermal expansion coefficient α_t can be calculated by(Yang *et al.* 2006)

$$P_t = P_1 V_1 + P_2 V_2 \tag{4}$$

where P_1 and P_2 are the corresponding material properties of Ge and Si.

3. Theoretical formulations and solution procedures

3.1 Theoretical formulations

It is noted that the ratio h/L is usually small so that the shear deformation is negligible. The total strain at the *x* direction is the sum of the mechanical strain ε_m and thermal strain ε_T, i.e., $\varepsilon_x = \varepsilon_m + \varepsilon_T$. For micro-beams undergoing moderately large deformation, von Karman type nonlinear strain ε_m is

$$\varepsilon_m = \frac{du}{dx} - z\frac{d^2w}{dx^2} + \frac{1}{2}\left(\frac{dw}{dx}\right)^2 \tag{5}$$

and $\varepsilon_T = \alpha(T - T_0) = \alpha\Delta T$, where ΔT is the temperature change, measured with respect to the initial temperature T_0. It is noted that this paper takes into account the uniform temperature change.

The strain energy of the micro-beam can be calculated from

$$V = \int_V \int_0^{\varepsilon_x} \sigma_x d\varepsilon_x dV = \int_V \frac{1}{2} E\left[\frac{du}{dx} - z\frac{d^2w}{dx^2} + \frac{1}{2}\left(\frac{dw}{dx}\right)^2 + \alpha\Delta T\right]^2 dV \tag{6}$$

The total transverse distributed force per unit length $q = F_e + F_c$ is measured positive in the direction of the deflection *w* and its potential energy is

$$W_q = \int_0^L \left(\int_0^w q dw\right) dx = \int_0^L \left[\int_0^w \left[\frac{\varepsilon_0 b V^2}{2(g_0 - w)^2} + \frac{0.65\varepsilon_0 V^2}{2(g_0 - w)} + \frac{\pi^2 \bar{h} c b}{240(g_0 - w)^4}\right] dw\right] dx \tag{7}$$

While the potential energy associated with the axial residual stress is

$$W_N = \frac{1}{2}\int_0^L N_a \left(\frac{dw}{dx}\right)^2 dx \tag{8}$$

Based on the principle of virtual work $\delta(W_q + W_N + V) = 0$, the governing equations can be expressed as

$$-k_1\left[\frac{3}{2}\left(\frac{dw}{dx}\right)^2\frac{d^2w}{dx^2}+\frac{d^2u}{dx^2}\frac{dw}{dx}+\frac{du}{dx}\frac{d^2w}{dx^2}\right]-k_2\frac{d^3u}{dx^3}+k_3\frac{d^4w}{dx^4}+\left(J_1\Delta T-N_a\right)\frac{d^2w}{dx^2}=q \tag{9a}$$

$$\frac{d}{dx}\left\{-k_1\left[\frac{du}{dx}+\frac{1}{2}\left(\frac{dw}{dx}\right)^2\right]+k_2\frac{d^2w}{dx^2}\right\}=0 \tag{9b}$$

The associate boundary conditions for fixed beam can be expressed as

$$u=0,\quad w=0,\quad dw/dx=0 \text{ at } x=(0 \text{ and } L) \tag{10}$$

in which

$$\rho_l=\int_{-\frac{h}{2}}^{\frac{h}{2}}\rho b dz,\ k_1=\int_{-\frac{h}{2}}^{\frac{h}{2}}\hat{E}b dz,\ k_2=\int_{-\frac{h}{2}}^{\frac{h}{2}}\hat{E}bz dz,\ k_3=\int_{-\frac{h}{2}}^{\frac{h}{2}}\hat{E}bz^2 dz,\ J_1=\int_{-\frac{h}{2}}^{\frac{h}{2}}\hat{E}\alpha b dz \tag{11}$$

where the effective modulus $\hat{E}=E$ for a narrow beam ($b<5h$) and $\hat{E}=E/\left(1-\nu^2\right)$ for a wide beam ($b\geq 5h$). Noted that for a homogenous micro-beam whose Young's modulus is a constant $k_2=0$, Eq. (9) reduces to the nonlinear governing equations for a homogenous micro-beam.

From Eq. (9) and boundary conditions (10), the motion equation for a FGM micro-beam subjected to temperature change accounting for geometric nonlinearity due to mid-plane stretching can be derived as

$$\left(k_3-\frac{k_2^2}{k_1}\right)\frac{d^4w}{dx^4}+\left(J_1\Delta T-N_a\right)\frac{d^2w}{dx^2}-\frac{d^2w}{dx^2}\int_0^L\left[\frac{k_1}{2L}\left(\frac{dw}{dx}\right)^2-\frac{k_2}{L}\frac{d^2w}{dx^2}\right]dx=q \tag{12}$$

To facilitate theoretical formulation and for generality of solutions, the following dimensionless quantities are introduced

$$\begin{gathered}k=k_3-k_2^2/k_1,\psi=\left(J_1\Delta T-N_a\right)L^2/k,\zeta_1=k_1g_0^2/2k,\\ \zeta_2=k_2g_0/k,\bar{w}_0=w_0/g_0,\bar{x}=x/L\end{gathered} \tag{13}$$

Hence, Eq. (12) can then be rewritten in dimensionless form as

$$\frac{d^4\bar{w}}{d\bar{x}^4}+\psi\frac{d^2\bar{w}}{d\bar{x}^2}-\frac{d^2\bar{w}}{d\bar{x}^2}\int_0^1\left[\xi_1\left(\frac{d\bar{w}}{d\bar{x}}\right)^2-\xi_2\frac{d^2\bar{w}}{d\bar{x}^2}\right]d\bar{x}=\bar{q} \tag{14}$$

The dimensionless distributed force is

$$\bar{q}(\bar{x})=\frac{R_c}{\left(1-\bar{w}\right)^4}+\frac{BV_0^{\,2}}{\left(1-\bar{w}\right)^2}+f\frac{BV_0^{\,2}}{\left(1-\bar{w}\right)} \tag{15}$$

where $R_c=\dfrac{\pi^2\bar{h}cbL^4}{240g_0^5k}$, $B=\dfrac{\varepsilon_0 bL^4}{2g_0^3k}$, $f=0.65\dfrac{g_0}{b}$. The non-dimensional boundary conditions are $\bar{w}=0,\ d\bar{w}/d\bar{x}=0$ at $\bar{x}$ = (0 and 1).

3.2 Solution procedures

Eq. (14) and the associated boundary conditions form a nonlinear ordinary differential equation system whose exact solution is not available. The DQ method is therefore used to solve this nonlinear system numerically. According to the DQM, the dimensionless deflection $\bar{w}$ and its derivatives at an arbitrary point $\bar{x}_i$ are approximated by (Shu 2000, Yang and Xiang 2007)

$$\bar{w}=\sum_{j=1}^{N}l_j(x)\bar{w}\left(x_j\right) \tag{16a}$$

$$\left.\frac{d^k\bar{w}}{d\bar{x}^k}\right|_{\bar{x}=\bar{x}_i}=\sum_{j=1}^{N}C_{ij}^{(k)}\bar{w}\left(x_j\right) \tag{16b}$$

where N is the total number of sampling points $\bar{x}_i$ unevenly distributed over the domain

$$\bar{x}_1=0.0,\ \bar{x}_2=0.001,\ \bar{x}_j=\frac{1}{2}\left[1-\cos\frac{\pi\left(j-2\right)}{N-3}\right],.....,\ \bar{x}_{N-1}=0.999,\ \bar{x}_N=1.0 \tag{17}$$

The weighting coefficients $C_{ij}^{(k)}$ are dependent on the distribution of sampling points only and can be calculated from recursive formulae

$$C_{ij}^{(1)}=\frac{\tilde{L}\left(\bar{x}_i\right)}{\left(\bar{x}_i-\bar{x}_j\right)\tilde{L}\left(\bar{x}_j\right)}\qquad i,j=1,2,...,N;i\neq j \tag{18a}$$

$$C_{ij}^{(1)} = C_{ii}^{(1)} = -\sum_{k=1}^{N} C_{ik}^{(1)} \qquad i, j = 1, 2, ..., N; i \neq k; i = j \tag{18b}$$

$$\tilde{L}(\bar{x}_i) = \prod_{j=1}^{N} (\bar{x}_i - \bar{x}_j) \quad i \neq j \tag{18c}$$

The higher-order weighting coefficient can then be obtained through matrix multiplication

$$C_{ij}^{(p+1)} = \sum_{k=1}^{N} C_{ik}^{(1)} C_{kj}^{(p)}, \quad (p = 1, 2, ...) \tag{19}$$

Applying DQ approximations to the governing Eq. (14), one has

$$\sum_{j=1}^{N} C_{ij}^{(4)} \bar{w}_j + \psi \sum_{j=1}^{N} C_{ij}^{(2)} \bar{w}_j - \sum_{j=1}^{N} C_{ij}^{(2)} \bar{w}_j \sum_{k=1}^{N} \left(C_{Nk}^{I} - C_{1k}^{I} \right) \left(\xi_1 \left(\sum_{j=1}^{N} C_{ij}^{(1)} \bar{w}_j \right)^2 - \xi_2 \sum_{j=1}^{N} C_{ij}^{(2)} \bar{w}_j \right) - \bar{q}_j = 0 \tag{20}$$

in which $\mathbf{C^I} = \left(\mathbf{C^{(1)}} \right)^{-1}$, and the distributed force per unit length can be expressed as

$$\bar{q}_j = \left[\frac{R_c}{\left(1 - \bar{w}_j\right)^4} + \frac{BV_0^{\,2}}{\left(1 - \bar{w}_j\right)^2} + f \frac{BV_0^{\,2}}{\left(1 - \bar{w}_j\right)} \right] \tag{21}$$

Accordingly, the boundary conditions become

$$\bar{w}_1 = 0, \quad \sum_{j=1}^{N} C_{2j}^{(1)} \bar{w}_j = 0, \quad \sum_{j=1}^{N} C_{N-1j}^{(1)} \bar{w}_j = 0, \quad \bar{w}_N = 0 \tag{22}$$

It should be noted that discarding the geometrically nonlinear terms in Eq. (20) leads to the following equations without the effect of geometric nonlinearity

$$\sum_{j=1}^{N} C_{ij}^{(4)} \bar{w}_j + \psi \sum_{j=1}^{N} C_{ij}^{(2)} \bar{w}_j - \bar{q}_j = 0 \tag{23}$$

Denoting the unknown static displacement by $\bar{\mathbf{w}} = \{\bar{w}_i\}^{\mathbf{T}}$ and the transverse force vector by $\bar{\mathbf{q}} = \{\bar{q}_i\}^{\mathbf{T}}$, the nonlinear and linear solutions of pull-in temperature variation ΔT_{PI}, pull-in voltage V_{PI} and pull-in deflection $\bar{w}_{PI}$, when exists, can be determined from Eqs. (20) and (22) and from Eqs. (22) and (23), respectively, following an iterative process below

(1) Assuming a trial voltage V_0, let $\bar{q}_i = (2\beta + f\beta + 4R_c)\bar{w}_i + \beta + f\beta + R_c \quad (i = 1, 2, ...N)$, which is the linear part in the Taylor series expansion of $\bar{q}_i$ .solve Eq. (23) and the associated boundary conditions (22) to find $\bar{\mathbf{w}}$ which is taken as the initial value $\bar{\mathbf{w}}^*$ to be used in the 1st round of iteration.

(2) Substituting $\bar{\mathbf{w}} = \bar{\mathbf{w}}^*$ into Eq. (21) to obtain a new force vector $\bar{\mathbf{q}}$ and expressing Eqs. (22) and (23) with this updated $\bar{\mathbf{q}}$ in matrix equation yields

$$\mathbf{K}\bar{\mathbf{w}} = \bar{\mathbf{q}} \tag{24}$$

where $\mathbf{K}$ is the "stiffness matrix". The solution of this equation is denoted as $\bar{\mathbf{w}}^{(1)}$.

(3) Update $\bar{\mathbf{w}}^*$ by $\bar{\mathbf{w}}^* = \bar{\mathbf{w}}^{(1)}$ and repeat step (2) to gain a new solution $\bar{\mathbf{w}}^{(2)}$.

(4) Repeat step (3) until the deflection converges to a prescribed error tolerance

$$\sqrt{\frac{\sum\left(\Delta\bar{\mathbf{w}}^{(k)}\right)^2}{\sum\left(\bar{\mathbf{w}}^{(k+1)}\right)^2}} \le 0.0001 \tag{25}$$

to obtain the linear deflection $\bar{\mathbf{w}}$ under the assumed trial voltage. $\Delta\bar{\mathbf{w}}^{(k)}$ is updated in each iteration by $\Delta\bar{\mathbf{w}}^{(k)} = \bar{\mathbf{w}}^{(k+1)} - \bar{\mathbf{w}}^{(k)}$.

(5) Increase the trial voltage V_0 and repeat steps (1)-(4) until the stiffness matrix $\mathbf{K}$ becomes singular or the iterative process fails to converge. The last trial voltage V_0 under which the deflection is solvable is the linear pull-in voltage V_{PI}, and the corresponding deflection is the linear pull-in deflection $\bar{\mathbf{w}}_{PI}$.

(6) In order to find the pull-in parameters with the effect of geometric nonlinearity, the initial iterative values $\bar{\mathbf{w}}^*$ needs to be put into Eq. (20) and its relevant boundary conditions. Repeat steps (3)-(5) to obtain the nonlinear pull-in parameters.

(7) Assuming a trial temperature variation ΔT and setting $V_0 = 0$, the "pull-in temperature variation" ΔT_{PI} and the corresponding pull-in deflection can be obtained according to the steps above.

4. Results and discussions

4.1 Validation example

Table 1 lists the material properties used in all of the examples except those in Table 2. The geometric parameters of the micro-beams are L = 410 μm, b = 100 μm, g_0 = 1.18 μm, h = 1.5 μm, unless stated otherwise. Since there are no experimental or theoretical results for FGM micro-beams, to validate the present analysis, the linear and nonlinear pull-in voltage results for a homogeneous micro-beam are compared with the experimental results and Ritz method-based solutions provided by Tilmans and Legtenberg (1994), in which E = 151GPa, the axial residual force Na = 0.0009 N. The convergence study is given in Table 2 where the pull-in voltages of clamped micro-beams of different lengths with varying total number of sampling points N are compared. It is seen that convergent results can be achieved when $N \ge 17$ for both linear and nonlinear analyses.

As can be observed, the Ritz method gives significantly lower pull-in voltages. The present analysis, however, yields results that are in much better agreement with the experimentally obtained pull-in voltages (Tilmans and Legtenberg 1994). The relative difference percentage between the experimental results and our theoretical pull-in voltages increases as the beam length

L increases and the percentage reaches 4.1% for L = 510 μm in linear analysis and only 2.6% in nonlinear analysis. This indicates that the geometric nonlinearity due to mid-plane stretching should be taken into account, particularly for long micro-beams (Abdel-Rahman *et al.* 2002, Batra *et al.* 2008a).

Table 2 Pull-in voltages (in V) of electrostatically actuated homogenous clamped micro-beams

L(μm)	N=13		N =17		N =19		Ritz Method (Tilmans and Legtenberg 1994)	Experiment (Tilmans and Legtenberg 1994)
	Linear	Nonlinear	Linear	Nonlinear	Linear	Nonlinear		
210	27.500	28.350	27.506	28.352	27.506	28.352	24.98	27.95
310	13.833	14.181	13.834	14.182	13.834	14.182	11.46	13.78
410	8.769	8.945	8.769	8.945	8.769	8.945	6.55	9.13
510	6.300	6.401	6.300	6.401	6.300	6.401	4.23	6.57

Table 3 Characteristics of 6 poly-SiGe graded micro-beam types

Type	V_2^T	γ	λ
1	0	128678	-546294
2	20	100879	-467207
3	40	74192	-377458
4	60	48533	-273720
5	80	23825	-150811
6	100	128678	-546294

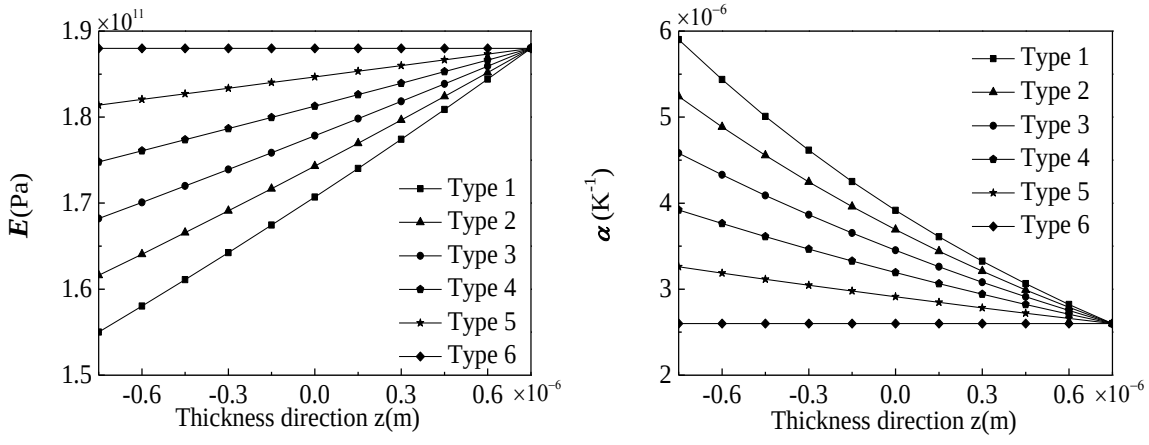

(a) Young's modulus (b) Thermal expansion coefficient

Fig. 2 Young's modulus and thermal expansion coefficient along thickness for the six FGM micro-beam

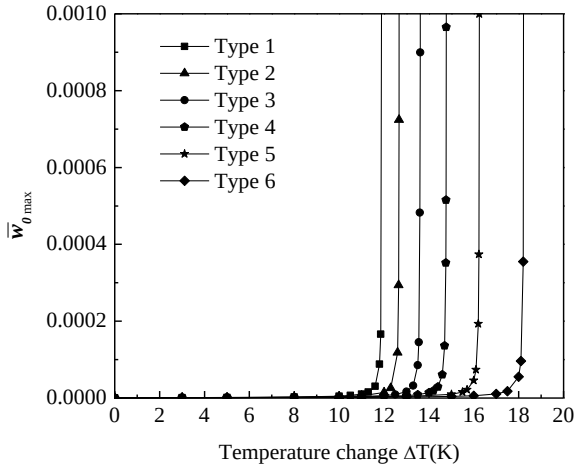

Fig. 3 Pull-in instability of poly-Si and poly-SiGe micro-beams for six types

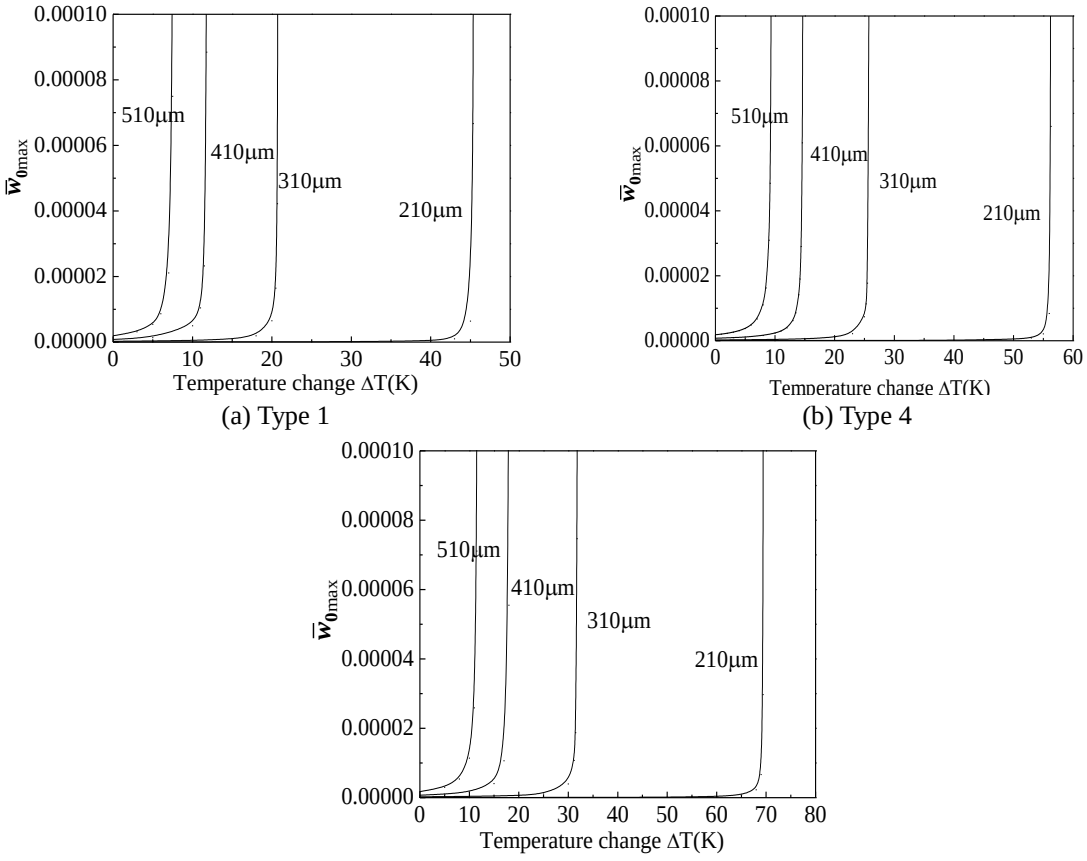

(a) Type 1 (b) Type 4

(c) Type 6

Fig. 4 The effect of beam length on the pull-in instability of poly-Si and poly-SiGe micro-beams for different beam types

4.2 FGM micro-beam under the influence of uniform temperature change

Table 3 and Fig. 2 gives the characteristics of 6 different types of FGM micro-beams, in which V_2^T denotes the volume fraction of Si among the top beam surface, the constants γ and λ can be worked out from Eqs. (3) and (4) (Mohammadi-Alasti *et al.* 2011).

The effect of uniform temperature change on the pull-in instability of poly-Si (Type 6) and poly-SiGe graded micro-beams (V=0V) is shown in Fig. 3, where $\bar{w}_{0\max}$ is the deflection of the middle point of the fixed FGM beam. In this and the following figures, solid lines and dashed lines denote the nonlinear and linear results, respectively. Fig. 3 shows that the deflection of the micro-beam increases with the growth of the temperature until a certain value. Then, the deflection increases sharply and the micro-beam loses its stability and spontaneously collapse or pulls in onto the fixed electrode. The micro-beam with a higher value of V_2^T has a larger "pull-in temperature variation" ΔT_{PI}, which are (11.91, 12.68, 13.62, 14.78, 16.26, 18.24) K for Types 1-6 respectively. This is because such a micro-beam contains more Si whose thermal expansion coefficient is smaller than that of Ge. However, the difference between linear and nonlinear results is insignificant as shown in Fig. 3.

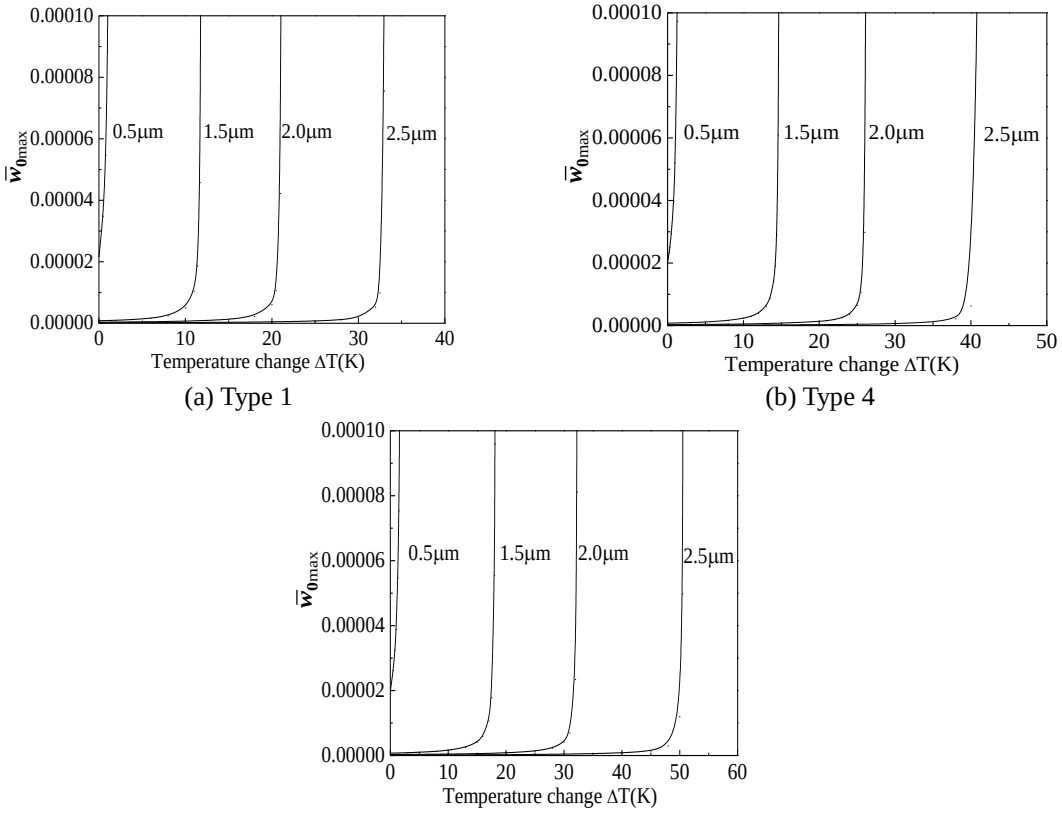

(a) Type 1

(b) Type 4

(c) Type 6

Fig. 5 The effect of beam thickness on the Pull-in instability of poly-Si and poly-SiGe micro-beams for different beam types

Plotted in Figs. 4 and 5 are curves showing the effect of FGM beam length and thickness on the $\bar{w}_{0\max}$ versus the unifrom temperature change for different micro-beam types, respectively. As expected, the micro-beam with smaller beam length and larger beam thickness has considerably larger "pull-in temperature variation" ΔT_{PI}. It is noted that increase tendency of ΔT_{PI} is more obvious with the decease of the beam length and growth of the beam thickness, especially in beam type with a higher value of V_2^T. Besides, another noteworthy phenomenon in Fig. 4 is $\bar{w}_{0\max}$ is not zero when ΔT=0 for micro-beam with h =0.5 μm , The reason is that the FGM micro-beam deflects under the effect of the Casimir force between the micro-beam and the fixed electrode.

The influence of axial residual force on the pull-in instability of poly-Si and poly-SiGe micro-beams for different beam types are dictated in Fig. 6, where N_a = 0 corresponds to a micro-beam without the action of axial residual stress. It is noted that as the axial residual stress N_a changes from a compressive force to a tensile force, the "pull-in temperature variation" ΔT_{PI} increases gradually for all the three beam types. These results imply that a negative axial residual stress can soften while the action of an axial residual tensile force can strengthen the FGM micro-beam.

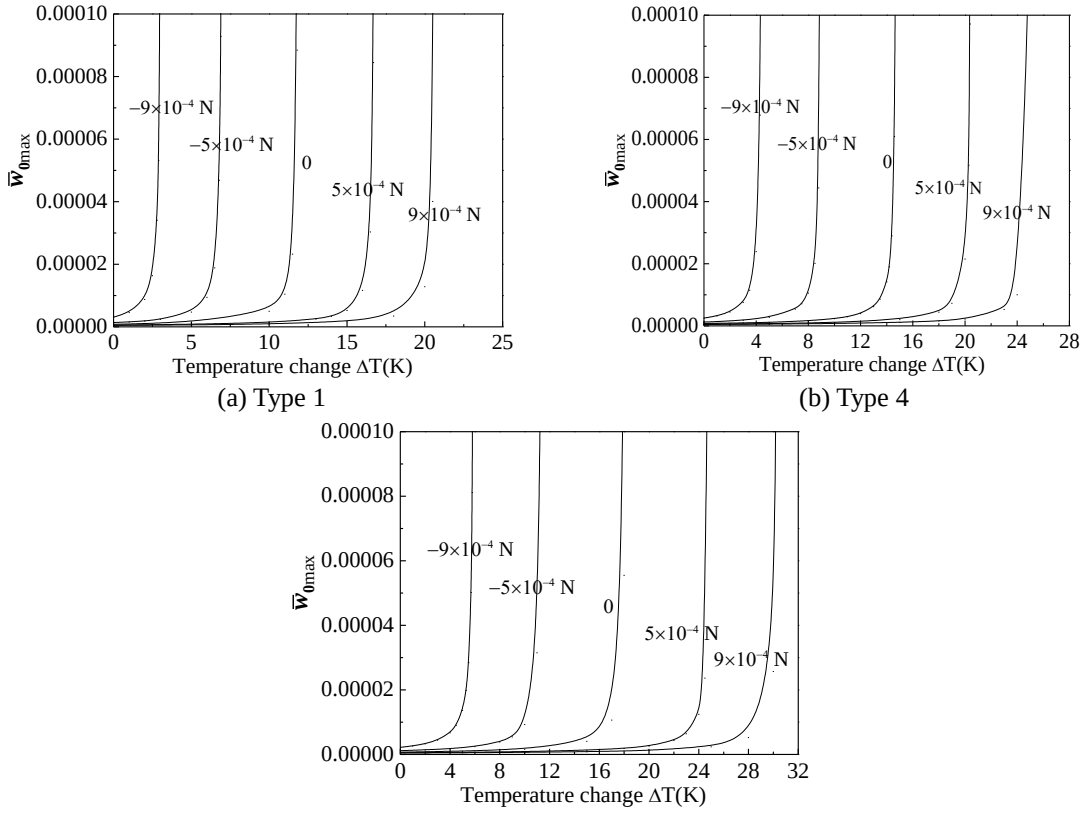

Fig. 6 The effect of axial force on the Pull-in instability of poly-Si and poly-SiGe micro-beams for different beam types

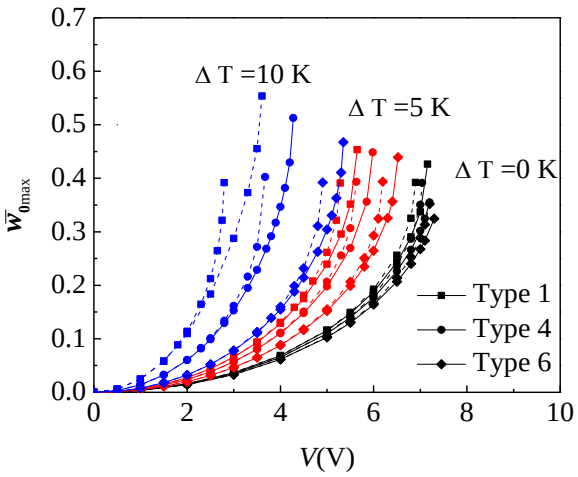

Fig. 7 Pull-in instability of poly-Si and poly-SiGe micro-beams subjected to electrostatic force

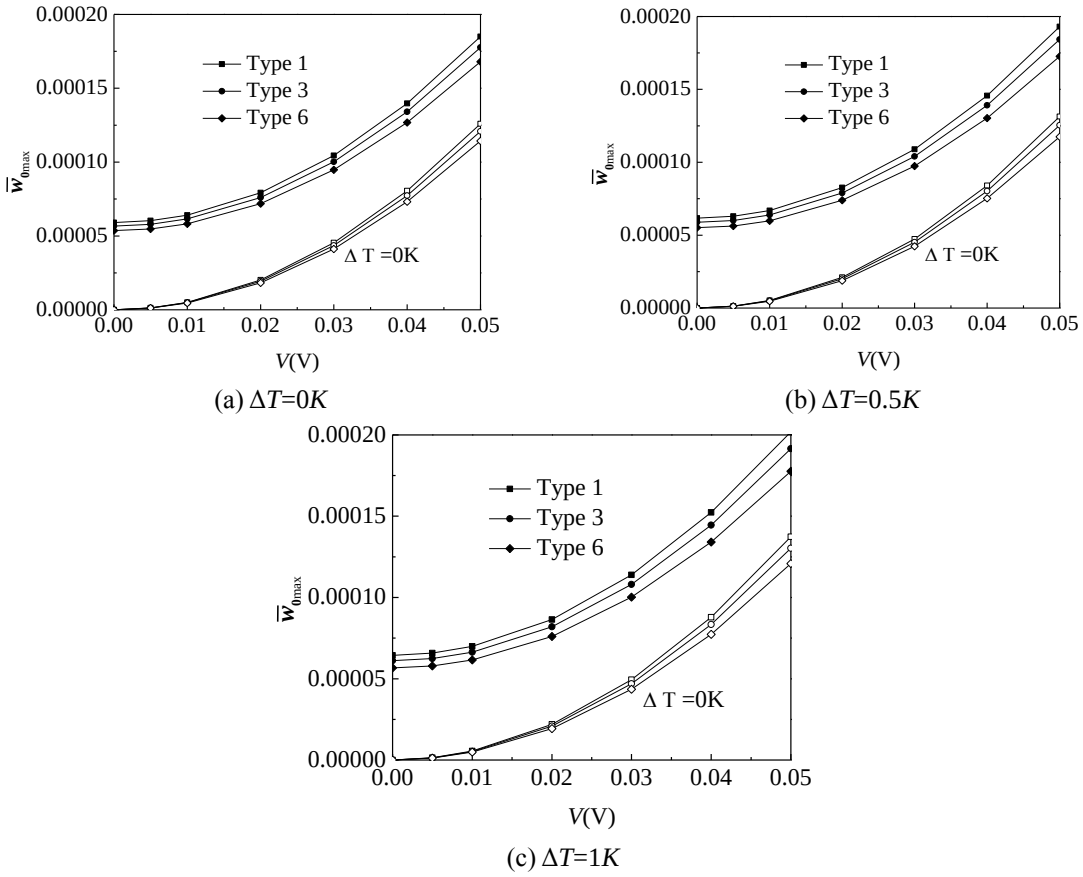

Fig. 8 The influence of Casimir force on the pull-in instability of poly-Si and poly-SiGe micro-beams

4.3 FGM micro-beam subjected to temperature change and nonlinear electrostatic force

Fig. 7 depicts the linear and nonlinear pull-in instability of the poly-Si and poly-SiGe micro-beams subjected to electrostatic force and temperature change ΔT=10 *K*. It is noted that neglecting the effect of geometric nonlinearity results in underestimated pull-in voltage and deflection. Both the linear and nonlinear pull-in voltage is increasing from Type 1 to Type 6. However, the nonlinear pull-in deflection is decreasing with the growth of V_2^T, but the linear pull-in deflection seems not to be impacted.

The intermolecular force is of prominent importance in some micro-switches where the micro-beam may collapse onto the fixed ground plane due to the Casimir force only (Batra *et al*. 2008b). Once the stiffness of the micro-beam decrease to some extent, the micro-beam may collapse even in the absence of an applied voltage and temperature change. As an example, we consider a micro-beam of length $L = 410\mu m$, aspect ratio b/L =0.244 and initial gap $g_0 = 0.5\mu m$. The effect of intermolecular Casimir force on the pull-in instability of different type of poly-SiGe graded micro-beams with varying temperature change ΔT is displayed in Fig. 8, where the curves plus hollow symbols denote the results without Casimir force, while the curves plus solid symbols represent the results considering the effect of Casimir force. As can be seen from the results, neglect of Casimir force may lead to a considerably higher pull-in voltage for all the beam types. The discrepancy tends to be smaller as temperature change ΔT increases. Besides, it is noted that the linear and nonlinear results are almost identical in this case.

5. Conclusions

The pull-in instability of poly-SiGe graded micro-beams under electrostatic and intermolecular Casimir forces, and temperature change is studied based on Euler-Bernoulli beam theory and von Karman type geometric nonlinearity. The governing equation and boundary conditions are solved numerically through DQ approximation to obtain the "pull-in temperature variation", pull-in voltage and pull-in deflection for fixed micro-beams. In this paper, the material property of the ploy-SiGe graded micro-beam varies along the thickness direction, and it can be indicated by exponential distribution model and Voigt model. A comprehensive study has been conducted to analyze the pull-in instability characteristics, it concluded that

- The poly-SiGe micro-beam deflects towards the ground electrode under the action of temperature change even without the application of the driving voltage V_0. the FGM micro-beam with a higher volume fraction ratio V_2^T exhibits less obvious thermal expansion phenomenon and can sustain a higher temperature change, in particular, for micro-beams with smaller beam length, larger beam thickness and positive axial residual stress N_a.
- The pull-in voltage decreases with the growth of the temperature when the micro-beam under the combined effect of driving voltage V_0 and temperature change. It is noteworthy that neglecting the effect of geometric nonlinearity results in underestimated pull-in voltage and deflection.
- It is noted that neglect of Casimir force may lead to a considerably higher pull-in voltage once the stiffness of the micro-beam decrease to some extent.

Acknowledgments

The research described in this paper was financially supported by the Science Foundation of China University of Petroleum, Beijing (No. YJRC-2013-32).

References

Abdel-Rahman, E.M., Younis, M.I. and Nayfeh, A.H. (2002), "Characterization of the mechanical behavior of an electrically actuated microbeam", *J. Micromech. Microeng.*, **12**(6), 759-766.

Batra, R.C., Porfiri, M. and Spinello, D. (2006), "Electromechanical model of electrically actuated narrow microbeams", *J. Microelectromech. S.*, **15**(5), 1175-1189.

Batra, R.C., Porfiri, M. and Spinello, D. (2008a), "Vibrations of narrow microbeams predeformed by an electric field", *J. Sound Vib.*, **309**(3-5), 600-612.

Batra, R.C., Porfiri, M. and Spinello, D. (2008b), "Reduced-order models for microelectromechanical rectangular and circular plates incorporating the Casimir force", *Int. J. Solids Struct.*, **45**(11-15), 3558-3583.

Birman, V. and Byrd, L.W. (2007), "Modeling and analysis of functionally graded materials and structures", *Appl. Mech. Rev.*, **60**(5), 195-216.

Carbonari, R.C., Silva, E.C.N. and Paulino, G.H. (2009), "Multi-actuated functionally graded piezoelectric micro-tools design: A multiphysics topology optimization approach", *Int. J. Numer. Meth. Eng.*, **77**(3), 301-336.

Craciunescu, C.M. and Wuttig, M. (2003), "New ferromagnetic and functionally graded shape memory alloys", *J. Optoelectron. Adv. M.*, **5**(1), 139-146.

Erdogan, F. and Wu, B.H. (1997), "The surface crack problem for a plate with functionally graded properties", *J. Appl. Mech.-T. ASME*, **64**(3), 449-456.

Fu, Y.Q., Du, H.J. and Zhang, S. (2003), "Functionally graded TiN/TiNi shape memory alloy films", *Mater. Lett.*, **57**(20), 2995-2999.

Ganguly, P. and Desiraju, G.R. (2008), "Van der Waals and polar intermolecular contact distances: Quantifying supramolecular synthons", *Chem.-Asian J.*, **3**(5), 868-880.

Gromova, M., Mehta, A., Baert, K. and Witvrouw, A. (2006), "Characterization and strain gradient optimization of PECVD poly-SiGe layers for MEMS applications", *Sens. Actuators A.*, **130**, 403-410. 2006.

Gupta, R.K. (1997), *Electrostatic Pull-in Test Structure Design for In-situ Mechanical Property Measurements of Microelectromechanical Systems*, Ph.D. dissertation, MIT, Cambridge, UK.

Hasanyan, D.J., Batra, R.C. and Harutyunyan, S. (2008), "Pull-in instabilities in functionally graded microthermoelectromechanical systems", *J. Therm. Stresses*, **31**(10), 1006-1021.

Huang, J.M., Liew, K.M., Wong, C.H., Rajendran, S., Tan, M.J. and Liu, A.Q. (2001), "Mechanical design and optimization of capacitive micro machined switch", *Sens. Actuators A.*, **93**(3), 273-285.

Jia, X.L., Yang, J. and Kitipornchai, S. (2010), "Characterization of FGM micro-switches under electrostatic and Casimir forces", *IOP Conf. Ser. Mater. Sci. Eng.*, **10**, 012018.

Jia, X.L., Yang, J. and Kitipornchai, S. (2011), "Pull-in instability of geometrically nonlinear micro-switches under electrostatic and Casmir forces", *Acta Mech.*, **218**(1-2), 161-174.

Lamoreaux, S.K. (2005), "The Casimir force: background, experiments, and applications", *Rep. Prog. Phys.*, **68**(1), 201-236.

Legtenberg, R. and Tilmans, H.A.C. (1994), "Electrostatically driven vacuum-encapsulated polysilicon resonators, Part I: Design and Fabrication", *Sens. Actuators A.*, **45**(1), 57-66.

Mobki, H., Rezazadeh, G., Sadeghi, M. and Vakili-Tahami, F. (2013), "A comprehensive study of stability in an electro-statically actuated micro-beam", *Int. J. Nonlinear Mech.*, **48**, 78-85.

Mohammadi-Alasti, B., Rezazadeh, G., Borgheei, A.M., Minaei, S. and Habibifar, R. (2011), "On the

mechanical behavior of a functionally graded micro-beam subjected to a thermal moment and nonlinear electrostatic pressure", *Compos. Struct.*, **93**(6), 1516-1525.

Nabian, A., Rezazadeh, G., Almassi, M. and Borgheei, A.M. (2013), "On the stability of a functionally graded rectangular micro-plate subjected to hydrostatic and nonlinear electrostatic pressures", *Acta Mech. Solida Sin.*, **26**(2), 205-220.

Sharafkhani, N., Rezazadeh, G. and Shabani, R. (2012), "Study of mechanical behavior of circular FGM micro-plates under nonlinear electrostatic and mechanical shock loadings", *Acta Mech.*, **223**(3), 579-591.

Shu, C. (2000), *Differential quadrature and its application in engineering: engineering applications*, Springer, Verlag, London.

Tilmans, H.A.C. and Legtenberg, R. (1994), "Electrostatically driven vacuum-encapsulated polysilicon resonators, Part II: Theory and performance", *Sensor Actuat. A-Phys.*, **45**(1), 67-84.

Witvrouw, A. and Mehta, A. (2005), "The use of functionally graded poly-SiGe layers for MEMS applications", *Mater. Sci. Forum.*, **492**, 255-260.

Yang, J., Liew, K.M. and Kitipornchai, S. (2005), "Second-order statistics of the elastic buckling of functionally graded rectangular plates", *Compos. Sci. Technol.*, **65**(7-8), 1165-1175.

Yang, J., Liew, K.M., Wu, Y.F. and Kitipornchai, S. (2006), "Thermo-mechanical post-bulkling of FGM cylindrical panels with temperature-dependent properties", *Int. J. Solids Struct.*, **43**(2), 307-324.

Yang, J. and Xiang, H.J. (2007), "Thermo-electro-mechanical characteristics of functionally graded piezoelectric actuators", *Smart Mater. Struct.*, **16**(3),784-797.